

Tracking vehicles using radar detections

J. Gunnarsson, L. Svensson
Chalmers University of Technology
Department of Signals and Systems
Göteborg, Sweden

joakim.gunnarsson@s2.chalmers.se
lennart.svensson@chalmers.se

L. Danielsson[†], F. Bengtsson^{††}
Volvo Car Corporation[†]
Volvo 3P^{††}
Göteborg, Sweden

ldanie25@volvocars.com
fredrik.bengtsson@volvo.com

Abstract—This paper is concerned with the problem of tracking vehicles using radar detections. In particular, we deal with problems where multiple detections are received from each target. According to recent studies, automotive radar sensors often receive detections from a discrete set of reflection centers. From these results, we develop a family of sensor models suitable for tracking. A significant difficulty in performing tracking using models from this family is that it involves solving a data association problem with a large number of association hypotheses. To reduce the complexity of this problem, we propose a framework where similar hypotheses are joined into groups. Following this approximation, basic data association algorithms can be implemented and initial studies using both simulated data and real measurements show a promising performance.

I. INTRODUCTION

In this paper we consider a vehicle tracking problem which, in contrast to the traditional point source assumption, allow for multiple detections to originate from each vehicle. By using the detections directly in the tracking filter, instead of forming an average measurement, valuable information regarding *e.g.* vehicle orientation can be extracted. To fully exploit the information in the detections, an accurate vehicle radar response model is required. A detailed sensor model is proposed in [1], which describes the radar response as if each vehicle was an extended object consisting of a fixed number of point- and plane reflectors. Even though this sensor model has many promising properties, it was originally developed for simulation purposes. In this paper, we suggest modifications and generalizations which result in a family of sensor models more suitable for tracking.

A significant difficulty with extended object tracking is data association, *i.e.* the task of handling uncertainty regarding the origin of the detections. Among recent contributions, several different approaches are suggested [2], [3], [4]. For instance, in [2], [3] the data associating problem is treated by incorporating the association hypothesis into the state vector; thus the output of the tracking filter is a joint posterior distribution of the state vector and the association hypothesis. The idea in [4] is instead to circumvent the data association problem by modelling the detections originating from each reflector as a non-homogenous Poisson point process. Both

approaches can be conveniently implemented using particle filter techniques.

Although the algorithms suggested in [2], [3], [4] are useful in many situations, they are not suitable for the tracking problem we attempt to solve using our family of sensor models. First, due to the limited resolution of the radar sensor, there is an uncertainty regarding which vehicle reflections are resolved and which are clustered. As a result, the number of association hypotheses is significantly larger than normal, and an approach similar to that in [2], [3] will be costly to implement. Second, the sensor model enables us to calculate the probability of receiving a specific number of detections from each vehicle. In fact, in many scenarios the number of vehicle detections are essentially known, and therefore not adequately modelled by a Poisson distribution. As a consequence, the non-homogenous Poisson point process assumption in [4] is inappropriate.

The main contributions in this article are suitable approximations which reduce the number of association hypotheses. Instead of associating detections with vehicle reflectors or reflector clusters, they are associated with reflector groups. Each group contains a set of reflectors, where each reflector is likely to be clustered with at least one other reflector in the group. The number of association hypotheses is often significantly reduced and we suggest a generalized version of the joint probabilistic data association (JPDA) technique [5], [6] to solve the problem.

The paper is organized as follows. In Section II the tracking problem is formalized and the necessary notation defined. Sections III, and IV present models required for solving the tracking problem, and in Section V we present the approximations for simplifying the data association problem. Finally, Section VI presents a tracking filter implementation and Section VII results, both based on simulations and real measurements.

II. PROBLEM FORMULATION

The objective in this article is to track a known number of vehicles moving in the vicinity of the host vehicle. Information regarding position and orientation of surrounding vehicles is collected using a radar sensor mounted on the host vehicle. The radar response is equidistantly sampled at times $t = \{t_0, t_1, \dots\}$, and we use k as notation for the corresponding discrete time index. For each k , the radar

This work was sponsored by the Swedish Intelligent Vehicle Safety Systems (IVSS) program, and is a part of the SEnsor Fusion for Safety Systems (SEFS) project.

provides M_k detections, which can either be false detections (clutter) or reflections from the vehicles. These detections are stored in a measurement vector \mathbf{y}_k .

For each vehicle, l , we define a state vector

$$\mathbf{z}_k^l = [\zeta_{x_k}^l \ \zeta_{y_k}^l \ \Psi_k^l \ v_k^l \ \dot{\Psi}_k^l \ \dot{v}_k^l]^T, \quad (1)$$

where $(\zeta_{x_k}^l, \zeta_{y_k}^l)$ is the position of vehicle l expressed in a Cartesian coordinate system situated at the host vehicle. As illustrated in Fig. 1, Ψ_k^l is the heading angle and v_k^l is the speed in the heading direction of vehicle l . The variables $\dot{\Psi}_k^l$ and \dot{v}_k^l are the time derivatives of Ψ_k^l and v_k^l respectively. The state vectors of all vehicles are stacked to form the complete state vector

$$\mathbf{z}_k = [(\mathbf{z}_k^1)^T \ (\mathbf{z}_k^2)^T \ \dots \ (\mathbf{z}_k^{N_v})^T]^T, \quad (2)$$

where N_v is the number of vehicles.

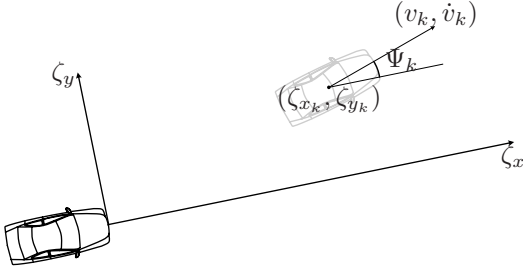


Fig. 1. Coordinate system used in this paper.

The aim of the tracking filter is to recursively calculate the posterior probability density function (pdf) $p(\mathbf{z}_k | \mathbf{Y}_{1:k})$. Using $p(\mathbf{z}_k | \mathbf{Y}_k)$ we can compute estimates and uncertainty measures of \mathbf{z}_k , based on all available measurements $\mathbf{Y}_{1:k} \triangleq \{\mathbf{y}_l, l = 1, \dots, k\}$. The calculation of $p(\mathbf{z}_k | \mathbf{Y}_{1:k})$ is feasible if we have knowledge regarding two models. The first model, the motion model, describes how the state vector evolves with time

$$\mathbf{z}_k = f_{k-1}(\mathbf{z}_{k-1}, \mathbf{e}_{k-1}), \quad (3)$$

and the second model, the measurement- or sensor model, gives the relation between the measurements and the state vector

$$\mathbf{y}_k = h_k(\mathbf{z}_k, \mathbf{w}_k). \quad (4)$$

In (3), \mathbf{e}_k is a noise process included to reflect model uncertainties and \mathbf{w}_k in (4) is a measurement noise process capturing both model uncertainties and measurement disturbances.

III. VEHICLE MOTION MODEL

A commonly used motion model for target tracking is the simplistic constant acceleration (CA) model, in which the lateral and longitudinal motions are decoupled. In related studies we suggest a more advanced modelling framework, [7], [8], to improve the model accuracy. For simplicity,

we here employ a simplified version of the well known bicycle model [9], which introduces a coupled motion in the lateral and longitudinal dimensions. By assuming that different vehicles move independently of each other we can describe their motions individually. In continuous time the state vector for vehicle l is denoted by $\mathbf{z}^l(t) = [\zeta_x^l(t) \ \zeta_y^l(t) \ \Psi^l(t) \ v^l(t) \ \dot{\Psi}^l(t) \ \dot{v}^l(t)]^T$, and the simplified continuous time bicycle model can be written as

$$\dot{\mathbf{z}}^l(t) = \begin{bmatrix} v^l(t) \cos(\Psi^l(t)) \\ v^l(t) \sin(\Psi^l(t)) \\ \dot{\Psi}^l(t) \\ \dot{v}^l(t) \\ 0 \\ 0 \end{bmatrix} + \begin{bmatrix} 0 \\ 0 \\ 0 \\ 0 \\ e_{\dot{\Psi}}^l(t) \\ e_{\dot{v}}^l(t) \end{bmatrix}, \quad (5)$$

where $e_{\dot{\Psi}}^l(t)$ and $e_{\dot{v}}^l(t)$ are zero-mean Gaussian noise processes with variances $\sigma_{\dot{\Psi}}^2$ and $\sigma_{\dot{v}}^2$ respectively. In the appendix, we present a discretized motion model which is used in our implementation.

IV. SENSOR MODEL

In this section, we describe and propose a family of measurement models for radar detections. The family is an adjustment and generalization of a model introduced in [1] for simulation of radar detections from a car. The objective with the modifications are mainly to make the models more suitable for tracking. A secondary purpose is to point out that the models may be applicable in many different settings, *e.g.* for various types of radars and vehicles.

A. Radar model

We consider a general radar sensor which delivers data in the form of detections. At time k we receive M_k^t detections originating from the vehicles, and M_k^c false detections, clutter. All detections are stored in the measurement vector

$$\mathbf{y}_k = [(\mathbf{d}_{k,1}^m)^T \ (\mathbf{d}_{k,2}^m)^T \ \dots \ (\mathbf{d}_{k,M_k}^m)^T]^T, \quad (6)$$

where $M_k = M_k^t + M_k^c$. Each detection contains the quantities,

$$\mathbf{d}_{k,i}^m = [r_{k,i}^m \ \dot{r}_{k,i}^m \ \phi_{k,i}^m]^T, \quad (7)$$

where $r_{k,i}^m$ is related to the range, $\dot{r}_{k,i}^m$ to the range rate, and $\phi_{k,i}^m$ to the azimuth angle of the object that gave rise to the detection. An important difficulty in our tracking problem, is that the observations are not labelled, *i.e.*, the origins of the detections are unknown. To deal with this issue, we introduce a data association vector $\mathbf{r}_k^{cc_k}$, of dimension $M_k \times 1$, parameterized by cc_k described further down in this section. This vector details the data association, such that the j^{th} element of $\mathbf{r}_k^{cc_k}$ specifies the origin of detection j . If, for instance, $\mathbf{r}_k^{cc_k}(j) = 0$ then $\mathbf{d}_{k,j}^m$ is clutter. Otherwise $\mathbf{r}_k^{cc_k}(j)$ is a positive integer that connects $\mathbf{d}_{k,j}^m$ to a particular vehicle reflector center, see below. Based on this notation, and an assumption of additive white Gaussian noise, the model for the target detections take a simple form,

$$\mathbf{d}_{k,j}^m = \mathbf{d}_{k, \mathbf{r}_k^{cc_k}(j)} + \mathbf{w}_{k, \mathbf{r}_k^{cc_k}(j)} \quad \forall j : \mathbf{r}_k^{cc_k}(j) \neq 0, \quad (8)$$

where $\mathbf{w}_{k, \mathbf{r}_k^{cc}(j)} \sim \mathcal{N}(\mathbf{0}, \Sigma_{k, \mathbf{r}_k^{cc}(j)})$. The clutter detections, on the other hand, are assumed uniformly distributed over the observations space, whereas the number of clutter detections is Poisson distributed with mean μ_c .

B. Vehicle radar response model

In addition to the radar model above, it is essential to also have a suitable model for the target response. Here we provide a brief description of the model suggested in [1], and explain the motivations for the proposed adjustments.

1) *Reflection center model*: Active radar sensors generally seek to illuminate a target and observe the echoes. According to the model in [1], the studied radar only receives reflections from a discrete set of points, so called *reflection centers*, on a vehicle. The different reflection centers are divided into two categories: point reflectors and plane reflectors. Figure 2 displays the configuration of reflectors suggested in [1], where the plane reflectors are modelled as circle sectors and point reflectors are placed in the vehicle wheel houses and corners. Attached to each point reflector is a visibility region, indicated by cones in Fig. 2, and the reflector can only give a reflection if the sensor is within this region. For plane reflectors, the radar only receives a reflection if the sensor is placed on the normal to the surface in that point. The reflecting point on a surface therefore depends on the position of the sensor, and may change over time.

Apart from the visibility, the probability of detection, P_d , for a reflector, with index i , also depends on its position in the sensor coordinate system. More specifically, a reflection is detected if the signal amplitude, $A_{k,i}$, is above a certain threshold. The amplitude model used in [1] is a deterministic function of the radar antenna pattern and the reflectors position and visibility.

Furthermore, given the state vector, reflector i has a deterministic position in the observation space¹

$$\mathbf{d}_{k,i} = D(\mathbf{z}_k, i). \tag{9}$$

Typically, $r_{k,i}$ and $\phi_{k,i}$ are simply the position of the reflector in the sensor coordinate system, whereas $\dot{r}_{k,i}$ is the time derivative of $r_{k,i}$. Note that the vehicle response model is rather general, and reflectors that yield, for instance, a different range rate are easily incorporated.

2) *Limited resolution*: As for all real sensors, the radar has limited resolution. Therefore, objects located too close in the measurement space render only one detection. To model this behavior, a resolution cell is used

$$\Delta_{\mathbf{d}} = [\Delta_r \ \Delta_{\dot{r}} \ \Delta_{\phi}]^T, \tag{10}$$

and two radar responses not separated more than Δ_r , $\Delta_{\dot{r}}$ and Δ_{ϕ} , in all three dimensions, yield a joint, clustered, detection. Unfortunately, the situation is more complicated for multiple reflections, and it is not easy to determine which reflection that are clustered. Following [1], the following algorithm is used to divide reflections into clusters:

¹From here on, the *position of a reflector* refers to the resulting three-dimensional vector in the observation space.

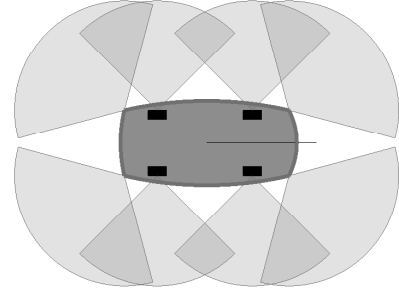


Fig. 2. The figure displays vehicle reflector centers with associated visibility regions.

- i) Find the reflector with the strongest amplitude, $A_{k,i}$.
- ii) Form a cluster by identifying the reflections which are within the resolution cell (positioned in $\mathbf{d}_{k,i}$).
- iii) Repeat i) and ii) with the remaining reflectors, until no reflectors are left.

We have previously stated that the measurement noise is additive and Gaussian, see Eq. (8). To describe the signal component, $\mathbf{c}_{k,i}$, of a cluster i , containing the reflectors i_1, \dots, i_N , we use the equation

$$\mathbf{c}_{k,i} = \sum_{l=1}^N w_{k,i_l} \mathbf{d}_{k,i_l}, \tag{11}$$

from [1], where

$$w_{k,i_l} = \frac{A_{k,i_l}}{\sum_{l=1}^N A_{k,i_l}}. \tag{12}$$

It is important to observe that, since the amplitudes are deterministic, so are both the set of clusters and their signal components.

3) *Stochastic amplitude*: From a tracking perspective, the model suggested in [1] and summarized above, is inappropriate as it neglects considerable uncertainties. Even given the state vector, it is typically unrealistic to claim that 1) we know if a reflector yields a detection or not, 2) the signal component in a cluster is deterministic and 3) even in complicated scenarios every cluster always contain the same reflectors. By employing such a model for tracking, one would seriously underestimate the posterior uncertainties, which, in turn, would lead to poor performance and high probabilities of losing the track. To avoid these problems we suggest a modified amplitude model, where the previous deterministic relation is replaced by a stochastic model. In this paper, we use a Rayleigh distribution to model the reflection amplitudes

$$A_{k,i} \sim \text{Rayleigh}(\sigma_{k,i}). \tag{13}$$

The expected value $E\{A_{k,i}\} = \sigma_{k,i} \sqrt{\pi/2}$ is set to the deterministic value of the amplitude in [1]. For a clustered reflection, containing signals from reflectors i_1, \dots, i_N , the amplitude is also Rayleigh distributed but with the parameter $\sigma_{k,i} = \sqrt{\sum_{l=1}^N \sigma_{k,i_l}^2}$.

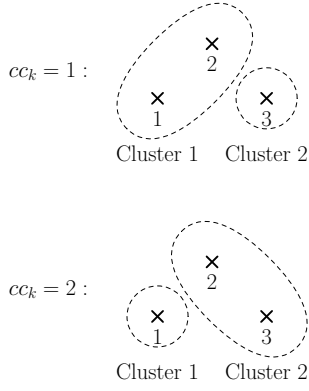


Fig. 3. Simple example of three reflectors and two different cluster constellations. The dashed line corresponds to a reflector cluster.

It is easy to see that through this simple modification, we will elude or, at least, alleviate all three model weaknesses mentioned above. As a reflection is detected if and only if the amplitude is larger than a threshold, we will find that the probability of detection, P_d , is now always smaller than 1. Moreover, the clustering algorithm depends on the amplitude, and the set of reflectors in a cluster may therefore also be random. Finally, the signal component, $\mathbf{c}_{k,i}$, in a cluster is also stochastic as the weights in (12) are functions of the amplitudes. Unfortunately, even though these properties are reasonable and desirable, in a sense, they also make the design of the tracking algorithm more delicate as they worsen the data association problem.

4) *Association hypotheses*: To evaluate the measurement likelihood it is convenient to condition on the data association vector, $\mathbf{r}_k^{cc_k}$, previously mentioned in Section IV-A. Having described the model in some detail we are now ready to clarify the interpretation of this vector.

The clustering algorithm above, can be used to divide the set of all visible reflectors into clusters. We refer to a description of all resulting clusters as a *cluster constellation*. Unfortunately, due to the stochastic nature of the amplitude, several different cluster constellations may be possible, even for a given vector \mathbf{z}_k . For notation, we construct a list of all possible constellations at time k , and introduce the variable cc_k as a pointer to the cluster constellations in the list. The total number of constellations in the list is denoted Mcc_k (and consequently $cc_k \in \{1, 2, \dots, Mcc_k\}$), and the number of clusters in constellation cc_k is $\mathbf{L}_k(cc_k)$. Now, if $\mathbf{r}_k^{cc_k}(j) = i$, the j^{th} detection is associated with the i^{th} cluster in constellation cc_k . To illustrate these concepts, Fig. 3 shows the two possible clutter constellations in a simple example. Clearly, $Mcc_k = 2$ and $\mathbf{L}_k = \begin{bmatrix} 2 & 2 \end{bmatrix}^T$ as each constellation contains two clusters.

We introduce the notation $\mathbf{c}_{k,i}^{cc_k}$ to describe the position of the i^{th} cluster in constellation cc_k . Similarly, we use $\mathbf{d}_{k,i_l}^{cc_k}$ as notation for the l^{th} reflector in cluster i . The measurement equation (8) can now be reformulated as

$$\mathbf{d}_{k,j}^m = \mathbf{c}_{k,\mathbf{r}_k^{cc_k}(j)}^{cc_k} + \mathbf{w}_{k,\mathbf{r}_k^{cc_k}(j)} \quad \forall j: \mathbf{r}_k^{cc_k}(j) \neq 0. \quad (14)$$

5) *A Gaussian signal model*: Most tracking algorithms rely on the possibility to evaluate the measurement likelihood,

$$p(\mathbf{y}_k | \mathbf{z}_k, \mathbf{r}_k^{cc_k}) = \prod_{j=1}^{M_k} p(\mathbf{d}_{k,j}^m | \mathbf{z}_k, \mathbf{r}_k^{cc_k}(j)), \quad (15)$$

at least, pointwise. In Section IV-A, we presented the pdf for clutter. Also, when cluster j in constellation cc_k only contains a single reflector, the distribution of $\mathbf{d}_{k,j}^m | \mathbf{z}_k, \mathbf{r}_k^{cc_k}(j)$ is given by Eq. (8) and (9). The aim in this section is therefore to describe the distribution for a detection associated with a cluster containing more than one reflector. In the remainder of this section, the state vector \mathbf{z}_k is always given but omitted for notational convenience.

For a cluster, the distribution of its position is defined by Eq. (11), (12) and (13), but is indeed very problematic to evaluate. The task is made even more intricate by the additive Gaussian noise in (14), forcing us to calculate the convolution between the noise and cluster distributions. Having said that, both difficulties are easily resolved by approximating $\mathbf{c}_{k,i}^{cc_k}$ as Gaussian distributed. The only remaining obstacle, then, is to calculate the first two moments of $\mathbf{c}_{k,i}^{cc_k}$.

Consider $\mathbf{c}_{k,i}^{cc_k}$ given by Eq. (11) and let overscore denote the expected value of stochastic variables, such that, e.g., $\bar{A}_{k,i} = E\{A_{k,i}\}$. Further, let $\Delta \mathbf{d}_{k,i_l}^{cc_k} = \mathbf{d}_{k,i_l}^{cc_k} - \bar{\mathbf{c}}_{k,i}^{cc_k}$, $\Delta w_{k,i_l} = w_{k,i_l} - \bar{w}_{k,i_l}$ and set $S_N = \sum_{l=1}^N A_{k,i_l}$. Clearly,

$$\bar{\mathbf{c}}_{k,i}^{cc_k} = \sum_{l=1}^N \bar{w}_{k,i_l} \mathbf{d}_{k,i_l}^{cc_k} \quad (16)$$

and straightforward manipulations yield that

$$\mathbf{C}_{k,i}^{cc_k} = \sum_{s,t=1}^N \Delta \mathbf{d}_{k,i_s}^{cc_k} \left(\Delta \mathbf{d}_{k,i_t}^{cc_k} \right)^T E\{\Delta w_{k,i_s} \Delta w_{k,i_t}\}, \quad (17)$$

where $\mathbf{C}_{k,i}^{cc_k} = \text{Cov}\{\mathbf{c}_{k,i}^{cc_k}\}$. Thus, the required quantities are \bar{w}_{k,i_l} and $\text{Cov}\{w_{k,i_s}, w_{k,i_t}\}$. As the moments of a Rayleigh variable are well known, approximations of these quantities are readily found through Taylor expansion,

$$w_{k,i_l} = \frac{A_{k,i_l}}{S_N} \approx \frac{\bar{A}_{k,i_l}}{\bar{S}_N} + \frac{A_{k,i_l}}{\bar{S}_N} - \frac{S_N \bar{A}_{k,i_l}}{\bar{S}_N^2}. \quad (18)$$

To conclude, the distribution of a clustered variable is approximated by a Gaussian distribution, which, for given data associations, results in a nonlinear Gaussian sensor model.

V. DATA ASSOCIATION APPROXIMATIONS

The primary difficulty with utilizing the above sensor model is to find a well performing and computationally feasible solution to the data association problem. To reduce the complexity of this problem, we try to lower the number of association hypotheses. As a first step, we join similar hypotheses into groups.

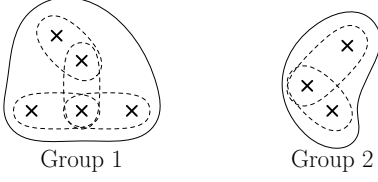


Fig. 4. The formation of two reflector groups.

A. Grouping of reflectors

Let a group be a set of reflectors, formed such that for every reflector i in the group, all reflectors sharing a cluster with reflector i are also included. Fig. 4 displays one scenario where two groups are formed from a set of reflectors. In the same figure, crosses indicate reflectors and dashed lines surround reflectors in a cluster. A suboptimal, but simplified, solution to the association problem is obtained by associating the detections to the reflector groups. By ignoring which cluster in a group that gave rise to a detection, the number of hypotheses are reduced substantially.

To lower complexity, each group is viewed as an entity which can generate multiple, and independent (this is an approximation), detections. The number of detections from group n at time k is given by $M_{k,n}^t$, and the signal component (the position) for the i^{th} of these is denoted $\mathbf{g}_{k,n}^{i(j)}$. The association of detections to groups is described by the association vector \mathbf{r}_k , which classifies the j^{th} detection as clutter if $\mathbf{r}_k(j) = 0$ and associates it to group n if $\mathbf{r}_k(j) = n$. Note that in difference to the previous association vector $\mathbf{r}_k^{cc_k}$, the current vector \mathbf{r}_k is independent of the cluster constellation. Since each group can render multiple detections, we define a vector \mathbf{i}_k which contains information about the number of detections associated with each group. For example, if $\mathbf{d}_{k,j}^m$ is the l^{th} detection to be associated with group n we have $\mathbf{i}_k(j) = l$. The measurement equation for detection j is now

$$\mathbf{d}_{k,j}^m = \mathbf{g}_{k,\mathbf{r}_k(j)}^{i_k(j)} + \mathbf{w}_{k,j} \quad \forall j : \mathbf{r}_k(j) \neq 0. \quad (19)$$

The vector $\mathbf{g}_{k,\mathbf{r}_k(j)}^{i_k(j)}$ is a random variable and to evaluate the likelihood $p(\mathbf{y}_k|\mathbf{z}_k, \mathbf{r}_k)$ we need an expression for the pdf $p(\mathbf{g}_{k,n}^{i_k(j)}|\mathbf{z}_k, \mathbf{r}_k)$. For cluster constellation cc_k , we let $\mathbf{c}_{k,l}^{cc_k}$ correspond to the position vector for the l^{th} cluster in group n , and $\mathbf{P}_n^{cc_k}(l)$ denote the detection probability for this cluster - a probability easily computed from the Rayleigh assumption in (13). If we assume that all cluster constellations are equally likely, we can express the distribution of $\mathbf{g}_{k,n}^{i_k(j)}|\mathbf{z}_k, \mathbf{r}_k$ as

$$p(\mathbf{g}_{k,n}^{i_k(j)}|\mathbf{z}_k, \mathbf{r}_k) = \sum_{cc_k=1}^{M_{cc_k}^n} \sum_{l=1}^{\mathbf{L}_k(cc_k)} \frac{\mathbf{P}_n^{cc_k}(l) p(\mathbf{c}_{k,l}^{cc_k} = \mathbf{g}_{k,n}^{i_k(j)}|\mathbf{z}_k, \mathbf{r}_k)}{M_{cc_k} \sum_{l=1}^{\mathbf{L}_k(cc_k)} \mathbf{P}_n^{cc_k}(l)}. \quad (20)$$

In practise, Eq. (20) is reduced by only considering constellations and clusters within the group.

To solve the data association problem, we need to calculate the probability for each group n to yield $M_{k,n}^t$ detections.

By introducing $M_{cc_k}^n$ as the number of different cluster constellations for group n , and again assuming that all cluster constellations are equally likely, we have

$$P(M_{k,n}^t|\mathbf{z}_k) = \frac{1}{M_{cc_k}^n} \sum_{cc_k=1}^{M_{cc_k}^n} P(M_{k,n}^t|\mathbf{z}_k, cc_k), \quad (21)$$

where $P(M_{k,n}^t|\mathbf{z}_k, cc_k)$ is easily calculated from $\mathbf{P}_n^{cc_k}(l)$.

To enable a simple implementation, e.g. using the Unscented Kalman Filter (UKF) or the Extended Kalman Filter (EKF) [3], we approximate $\mathbf{g}_{k,n}^{i_k(j)}$ as a normal distribution. The expected value, $\bar{\mathbf{g}}_{k,n}^{i_k(j)} = E\{\mathbf{g}_{k,n}^{i_k(j)}|\mathbf{z}_k\}$ is given by

$$\bar{\mathbf{g}}_{k,n}^{i_k(j)} = \sum_{cc_k=1}^{M_{cc_k}^n} \sum_{l=1}^{\mathbf{L}_k(cc_k)} \frac{\mathbf{P}_n^{cc_k}(l) \bar{\mathbf{c}}_{k,l}^{cc_k}}{M_{cc_k} \sum_{l=1}^{\mathbf{L}_k(cc_k)} \mathbf{P}_n^{cc_k}(l)} \quad (22)$$

and the second moment, $\mathbf{C}_{k,n} = E\{(\mathbf{g}_{k,n}^{i_k(j)} - \bar{\mathbf{g}}_{k,n}^{i_k(j)})(\mathbf{g}_{k,n}^{i_k(j)} - \bar{\mathbf{g}}_{k,n}^{i_k(j)})^T|\mathbf{z}_k\}$ by

$$\mathbf{C}_{k,n} = \sum_{cc_k=1}^{M_{cc_k}^n} \sum_{l=1}^{\mathbf{L}_k(cc_k)} \frac{\mathbf{P}_n^{cc_k}(l) (\mathbf{C}_{k,l}^{cc_k} + (\bar{\mathbf{g}}_{k,n} - \bar{\mathbf{c}}_{k,l}^{cc_k})(\bar{\mathbf{g}}_{k,n} - \bar{\mathbf{c}}_{k,l}^{cc_k})^T)}{M_{cc_k} \sum_{l=1}^{\mathbf{L}_k(cc_k)} \mathbf{P}_n^{cc_k}(l)}. \quad (23)$$

B. Joint Probabilistic Data Association

Based on the concept of grouping, there are many well known techniques that can be exploited to solve the data association problem [6]. In this article, we employ a generalized version of the *Joint Probabilistic Data Association* (JPDA) algorithm [5], [6], which, in difference to standard JPDA, can associate multiple detections to each group. In addition, gating is used for each group, to remove unlikely detections [6].

For group n , we denote the collection of all detections inside its gate by \mathbf{y}_k^n . Given knowledge regarding the maximum number of detections generated by group n , it is possible to construct the set of all *local hypotheses*, i.e., the set of all feasible associations between \mathbf{y}_k^n and group n . By combining local hypotheses from all groups in an admissible fashion (such that each detection in \mathbf{y}_k is associated to precisely one group, or classified as clutter) we obtain a *global hypothesis*, described by the vector \mathbf{r}_k . The set of all such hypotheses are denoted \mathcal{R}_k .

The idea with JPDA is to update the track using all association hypotheses, at time k , weighted by their probabilities,

$$p(\mathbf{z}_k|\mathbf{Y}_{1:k}) = \sum_{\mathbf{r}_k \in \mathcal{R}_k} p(\mathbf{z}_k|\mathbf{r}_k, \mathbf{Y}_{1:k}) P\{\mathbf{r}_k|\mathbf{Y}_{1:k}\}. \quad (24)$$

To make the implementation practical, the posterior distribution, $p(\mathbf{z}_k|\mathbf{Y}_{1:k})$, is approximated by a Gaussian distribution for all times. For each \mathbf{r}_k , the posterior mean and covariance of $p(\mathbf{z}_k|\mathbf{r}_k, \mathbf{Y}_{1:k})$ are easily approximated, e.g., using the UKF or the EKF. The latter part of (24) can be expressed as

$$P\{\mathbf{r}_k|\mathbf{Y}_{1:k}\} \propto p(\mathbf{y}_k|\mathbf{r}_k, \mathbf{Y}_{1:k-1}) P\{\mathbf{r}_k|\mathbf{Y}_{1:k-1}\}, \quad (25)$$

where the distribution

$$p(\mathbf{y}_k | \mathbf{r}_k, \mathbf{Y}_{1:k-1}) = \int p(\mathbf{y}_k | \mathbf{r}_k, \mathbf{z}_k) p(\mathbf{z}_k | \mathbf{Y}_{1:k-1}) d\mathbf{z}_k, \quad (26)$$

is obtained from the EKF, see Section VI. However, to deal with the data association prior, $P\{\mathbf{r}_k | \mathbf{Y}_{1:k-1}\}$, requires some new notation.

Naturally, the data association vector, \mathbf{r}_k , provides perfect knowledge regarding the number of clutter detections, M_k^c , and the number of detections from group n , $M_{k,n}^t$. Hence, the prior probability for the association vector in (24) is

$$P\{\mathbf{r}_k | \mathbf{Y}_{1:k-1}\} = P\{\mathbf{r}_k | M_k^t, M_k^c\} P\{M_k^c\} P\{M_{k,n}^t | \mathbf{Y}_{1:k-1}\}, \quad (27)$$

where $M_k^t = [M_{k,1}^t \ \dots \ M_{k,M_k^g}^t]^T$ and M_k^g is number of groups. Among these factors, we have that $P\{M_k^c\} = (\mu V)^{M_k^c} \exp(-\mu V) / M_k^c!$ and

$$P\{\mathbf{r}_k | M_k^t, M_k^c\} = \prod_{n=1}^{M_k^g} \binom{M_k - \sum_{m=1}^{n-1} M_{k,m}^t}{M_{k,n}^t}^{-1}. \quad (28)$$

Finally, we apply the approximation

$$P\{M_{k,n}^t | \mathbf{Y}_{1:k-1}\} \approx \prod_{n=1}^{M_k^g} P\{M_{k,n}^t | \mathbf{z}_k = \hat{\mathbf{z}}_{k|k-1}\} \quad (29)$$

where $P\{M_{k,n}^t | \mathbf{z}_k\}$ was described in Section V-A, and $\hat{\mathbf{z}}_{k|k-1} = E\{\mathbf{z}_k | \mathbf{Y}_{1:k-1}\}$ is calculated in the EKF, see Section VI.

VI. FILTER IMPLEMENTATION

As indicated above, we combine the proposed JPDA solution with an EKF implementation, to obtain a well performing, but simple, algorithm. To find the desired distribution $p(\mathbf{z}_k | \mathbf{Y}_{1:k})$, the above JPDA algorithm only requires the distributions $p(\mathbf{z}_k | \mathbf{r}_k, \mathbf{Y}_{1:k})$, $p(\mathbf{y}_k | \mathbf{r}_k, \mathbf{Y}_{1:k-1})$ and the prediction $\hat{\mathbf{z}}_{k|k-1}$. All these are approximated in the EKF framework.

A. The EKF components

The EKF filter is based on linearized versions of the motion model (3) and the measurement model (4). Given the discrete motion model in the appendix, the linearized version of (3) is easily derived. Regarding the measurement model, all detections are independent, conditioned on \mathbf{r}_k and \mathbf{z}_k . It is therefore sufficient to linearize the sensor model for a scenario with only one detection, as the measurement updates can be performed sequentially over $\mathbf{d}_{k,i}^m$.

Suppose a detection, $\mathbf{d}_{k,j}^m$, is associated with group n , such that the sensor model is given by (19)². The noise covariance matrix, in this model, is the sum of two components: the covariance matrix for $\mathbf{w}_{k,j}$ and the covariance, $\mathbf{C}_{k,n}$, for $\mathbf{g}_{k,r_k}^{i_k(j)}$. Furthermore, influence of the state vector enters through (22), as the cluster means $\bar{\mathbf{c}}_{k,l}^{cc_k}$ depend on the reflector positions. To simplify the linearization of (9), we

²Of course, if the detection is a clutter observation the measurement update is not performed.

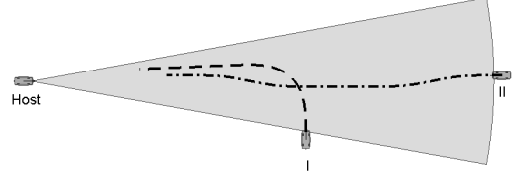


Fig. 5. Simulated trajectories used for scenario I and scenario II, respectively. In scenario I, the vehicle starts at a speed of 18 km/h and temporarily decelerates while turning. In scenario II the vehicle performs two lane change manoeuvres at a constant speed of 32 km/h.

assume that the reflectors move precisely like \mathbf{z}_k , in real coordinates. Using the Jacobian for $\nabla_{\mathbf{z}_k} D(\mathbf{z}, i)$, in (9), we can linearize (16) and thereby express $\nabla_{\mathbf{z}_k} \bar{\mathbf{g}}_{k,r_k}^{i_k(j)}$ required in the EKF.

Details regarding the EKF equations can be found, e.g., in [3], and are omitted here for brevity.

VII. NUMERICAL EXAMPLES

In this section we evaluate our filter both on simulated and measured data. The measurements are collected using a 77 GHz Frequency Shift Keying (FSK) radar (AC10) from TRW. For comparison we implement a reference EKF employing the probabilistic data association (PDA) algorithm [10]. In PDA, at most one measurement can originate from the object and the presence of multiple measurements is modelled as clutter. The reference filter compensates for offset errors using the geometry of the vehicle and its estimated position. A filter update rate of 40ms (equal to the measurement rate of the FSK radar) is used both for simulated and measured data.

A. Simulations

The tracking performance is evaluated for two trajectories displayed in Fig. 5. Both trajectories are generated using our motion model (5) driven by a known input signal. Detections are then generated from the sensor model described in Section IV with $\Delta_{\mathbf{d}} = [1m, 0.1m/s, 1^\circ]^T$ and $\Sigma_k = \text{diag}\{(\sqrt{\mathbf{z}_k(1)^2 + \mathbf{z}_k(2)^2}/60)^2, 0.5^2, (0.3\pi/180)^2\}$. The sensor model is used without the approximations suggested in the filtering framework. Hence, we use a more detailed model to generate data compared to the filter implementation. In addition to the detections generated from the simulated vehicle we add clutter with an intensity $\lambda = 0.07$.

For both scenarios, the filters are initiated at the true state vector, and the noise variances are set to $\sigma_{\Psi}^2 = 1/16$, $\sigma_v^2 = 9$. In Fig. 6, the result of 100 Monte Carlo simulations is displayed. The top two graphs correspond to scenario I, and the other two to scenario II. In the first scenario we observe a significantly improved performance compared to the reference filter, whereas in the second scenario the difference is much smaller. The reason for the variations in performance is related to the number of visible reflectors on the vehicle. The ability to utilize more than one measurement from a single target is greatly improved using the extended

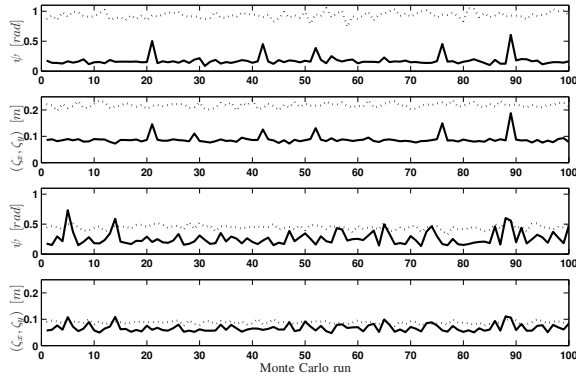


Fig. 6. Root mean square error (RMSE) for position $(\zeta_{x_k}, \zeta_{y_k})$ and heading Ψ_k for scenario I and II

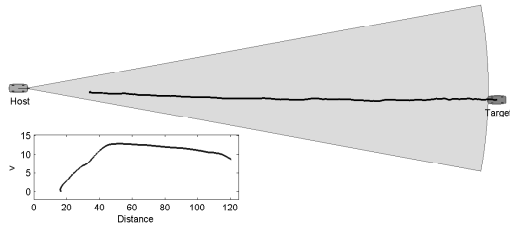


Fig. 7. Tracking performance on measured radar data.

object representation. As opposed to the PDA, which will be less certain when the number of measurements increase, the proposed filter is able to exploit the information they contain.

B. Results using measurement data

The FSK radar used to collect measurements, separates objects based on their range rate only, *i.e.* $\Delta_{\mathbf{d}} = [\infty \ v_{res} \ \infty]$. The test scenario consist of a car driving at nearly constant speed at 40 km/h towards a truck, stopping just in front of the sensor. In Fig. 7, the estimated trajectory is presented, and the velocities at certain distances are shown in a sub-figure. The trajectory estimated by the filter, well coincides with the actual path driven by the vehicle.

APPENDIX DISCRETIZED MOTION MODEL

A discrete motion model is derived under the assumption that the noise terms $e_{\dot{\Psi}}^l(t)$ and $e_{\dot{v}}^l(t)$ are constant in the interval (t_{k-1}, t_k) . For the elements Ψ_k^l , v_k^l , $\dot{\Psi}_k^l$ and \dot{v}_k^l , the discrete time model will be linear and take the form

$$\begin{bmatrix} \Psi_k^l \\ v_k^l \\ \dot{\Psi}_k^l \\ \dot{v}_k^l \end{bmatrix} = \begin{bmatrix} 1 & T & 0 & 0 \\ 0 & 1 & 0 & T \\ 0 & 0 & 1 & 0 \\ 0 & 0 & 0 & 1 \end{bmatrix} \begin{bmatrix} \Psi_{k-1}^l \\ v_{k-1}^l \\ \dot{\Psi}_{k-1}^l \\ \dot{v}_{k-1}^l \end{bmatrix} + \begin{bmatrix} T^2/2 & 0 \\ 0 & T^2/2 \\ T & 0 \\ 0 & T \end{bmatrix} \begin{bmatrix} e_{\dot{\Psi}_{k-1}}^l \\ e_{\dot{v}_{k-1}}^l \end{bmatrix}, \quad (30)$$

where $T = t_k - t_{k-1}$. The remaining two elements in the state vector $(\zeta_{x_k}^l, \zeta_{y_k}^l)$ becomes non-linear and can be written as

$$\begin{aligned} \zeta_{x_k}^l &= \zeta_{x_{k-1}}^l + \cos(\Psi_{k-1}^l) \left(v_{k-1}^l T + \frac{\dot{v}_{k-1}^l T^2}{2} + \frac{e_{\dot{v}_{k-1}}^l T^3}{6} \right) \\ &\quad - \sin(\Psi_{k-1}^l) \left(\frac{v_{k-1}^l \dot{\Psi}_{k-1}^l T^2}{2} + \frac{(v_{k-1}^l e_{\dot{\Psi}_{k-1}}^l + 2\dot{v}_{k-1}^l \dot{\Psi}_{k-1}^l) T^3}{6} \right. \\ &\quad \left. + \frac{(e_{\dot{v}_{k-1}}^l \dot{\Psi}_{k-1}^l + \dot{v}_{k-1}^l e_{\dot{\Psi}_{k-1}}^l) T^4}{8} + \frac{e_{\dot{v}_{k-1}}^l e_{\dot{\Psi}_{k-1}}^l T^5}{20} \right) \end{aligned} \quad (31)$$

$$\begin{aligned} \zeta_{y_k}^l &= \zeta_{y_{k-1}}^l + \sin(\Psi_{k-1}^l) \left(v_{k-1}^l T + \frac{\dot{v}_{k-1}^l T^2}{2} + \frac{e_{\dot{v}_{k-1}}^l T^3}{6} \right) \\ &\quad + \cos(\Psi_{k-1}^l) \left(\frac{v_{k-1}^l \dot{\Psi}_{k-1}^l T^2}{2} + \frac{(v_{k-1}^l e_{\dot{\Psi}_{k-1}}^l + 2\dot{v}_{k-1}^l \dot{\Psi}_{k-1}^l) T^3}{6} \right. \\ &\quad \left. + \frac{(e_{\dot{v}_{k-1}}^l \dot{\Psi}_{k-1}^l + \dot{v}_{k-1}^l e_{\dot{\Psi}_{k-1}}^l) T^4}{8} + \frac{e_{\dot{v}_{k-1}}^l e_{\dot{\Psi}_{k-1}}^l T^5}{20} \right). \end{aligned} \quad (32)$$

REFERENCES

- [1] M. Bühren and B. Yang, "Simulation of automotive radar target lists using a novel approach of object representation," in *IEEE Intelligent Vehicles Symposium (IV)*, Tokyo, Japan, June 2006.
- [2] J. Vermaak, N. Ikoma, and S. Godsill, "Sequential monte carlo framework for extended object tracking," *IEE Proceedings on Radar, Sonar and Navigation*, vol. 153, pp. 353–363, October 2005.
- [3] B. Ristic, S. Arulampalam, and N. Gordon, *Beyond the Kalman filter: particle filters for tracking applications*. Artech House, 2004.
- [4] K. Gilholm, S. J. Godsill, S. Maskell, and D. J. Salmond, "Poisson models for extended target and group tracking," *SPIE*, October 2005.
- [5] T. Fortmann, Y. Bar-Shalom, and M. Scheffe, "Sonar tracking of multiple targets using joint probabilistic data association," *IEEE Journal of Oceanic Engineering*, vol. 8, July 1983.
- [6] S. Blackman and R. Popoli, *Design and analysis of modern tracking systems*. Norwood, MA: Artech House, 1999.
- [7] L. Svensson and J. Gunnarsson, "A new motion model for tracking of vehicles," in *14th IFAC Symposium on System Identification*, Newcastle, Australia, March 2006.
- [8] J. Gunnarsson, L. Svensson, F. Bengtsson, and L. Danielsson, "Joint driver intention classification and tracking of vehicles," in *Nonlinear Statistical Signal Processing Workshop 2006*, Cambridge, UK, September 2006.
- [9] N. Kaempchen, K. Weiss, M. Schaefer, and K. Dietmayer, "Imm object tracking for high dynamic driving maneuvers," in *Intelligent Vehicles Symposium, 2004 IEEE*, June 2004.
- [10] Y. Bar-Shalom and E. Tse, "Tracking in a cluttered environment with probabilistic data association," *Automatica*, vol. 11, September 1975.